Chinese Chemical Letters 35 (2024) 109281

Contents lists available at ScienceDirect

Chinese Chemical Letters

journal homepage: www.elsevier.com/locate/cclet

A novel fused bi-macrocyclic host for sensitive detection of $Cr_2O_7^{2-}$ based on enrichment effect

Ting-Ting Huang[a], Jin-Fa Chen[a], Juan Liu[b], Tai-Bao Wei[a], Hong Yao[a], Bingbing Shi[a], Qi Lin[a,*]

[a] Key Laboratory of Eco-functional Polymer Materials of the Ministry of Education, Key Laboratory of Eco-environmental Polymer Materials of Gansu Province, College of Chemistry and Chemical Engineering, Northwest Normal University, Lanzhou 730070, China
[b] Key Laboratory of Environment-Friendly Composite Materials of the State Ethnic Affairs Commission, Gansu Provincial Biomass Function Composites Engineering Research Center, College of Chemical Engineering, Northwest Minzu University (Northwest University for Nationalities), Lanzhou 730000, China

ARTICLE INFO

Article history:
Received 4 August 2023
Revised 27 October 2023
Accepted 6 November 2023
Available online 9 November 2023

Keywords:
Pillar[5]arene
Bi-macrocyclic
Detection of $Cr_2O_7^{2-}$
DFT
The enrichment effect

ABSTRACT

Improving the highly selective and sensitive binding of chemosensor to target guest is always very challenging. In order to solve this issue, herein, the enrichment effect was introduced into the design of chemosensor molecule. A novel bi-fused-macrocyclic host molecule **BPN1** was synthesized by bridging a pillar[5]arene and a naphthalene diimide (**NDI**) group through hydrogen-bond-rich chain. In the **BPN1**, the naphthalimide side ring is outside the cavity of the pillar[5]arene. In addition, Cr(VI) greatly threat human health and the environment due to its severe toxicity, and it is very important to develop effective chemosensor for sensitive and selective detection of $Cr_2O_7^{2-}$ or its ion pairs. In this paper, the novel bi-fused-macrocyclic host molecule **BPN1** can recognize $Cr_2O_7^{2-}$ with high selectivity and sensitivity. The mechanism of **BPN1** recognition of $Cr_2O_7^{2-}$ was studied through experiments and density functional theory (DFT), the results show that **BPN1** could supply enrichment effect to bind $Cr_2O_7^{2-}$ through multiple weak interactions such as hydrogen bonds and anion-π, and achieve highly sensitive and selective detection of $Cr_2O_7^{2-}$. It is a significant and feasible strategy for improve high selectivity and sensitivity of host to specific objects by using the enrichment effect of fused bi-macrocyclic.

The development of new macrocyclic hosts has always been a hotspot in supramolecular chemistry due to its wide range of applications such as in sensors [1,2], self-assembled materials [3–5], and molecular machines [6]. By far, many macrocyclic hosts, including crown ethers [7,8], cyclodextrins [9], calixarenes [10], cucurbiturils [11,12], pillararenes [13–21], *etc.*, have been successfully developed and widely used. However, there is still a huge demand for novel macrocyclic hosts to supply more exact and effective binding for various target guests to achieve specific functions. To address this pressing need, a variety of efforts have been carried out in different ways, including modifying the existing macrocycle, developing new macrocycles, bi-macrocyclic hosts, and cages to adapt the target guests and supply exact binding [22–25]. All these approaches have their respective merits, while fused bi-macrocyclic hosts can supply two macrocycles to bind target guests. Moreover, the two macrocycles of the fused bi-macrocyclic host can supply an enrichment effect through the collaboration of the two cycles to bind more complicated guests or construct a more sophisticated supramolecular functional system [14,26–29]. Therefore, developing a novel fused bi-macrocyclic host and deeply investigating its host-guest interaction properties are very interesting and important.

As is well known, heavy metal ion contamination is one of the most severe environmental problems, which poses a great threat to the survival of living species [30–33]. For instance, Cr(VI) and its oxyanions such as dichromate ions ($Cr_2O_7^{2-}$) are widely utilized in chemical engineering including metallurgy, metal plating, pigments, and other fields [34,35], while Cr(VI) featured high toxicity, carcinogenicity, and so on. Moreover, since dichromate ($Cr_2O_7^{2-}$) is the most common source of chromium(VI), on the basis of the existing supramolecular strategies to recognize $Cr_2O_7^{2-}$ [36–39], it is very important to develop new strategy that effectively bind $Cr_2O_7^{2-}$ to improve the sensitivity and selectivity of $Cr_2O_7^{2-}$ or its ion pairs. Significantly, the rapid development of macrocyclic chemistry supplied a bright opportunity to improve the sensing sensitivity and selectivity.

* Corresponding author.
E-mail address: linqi2004@126.com (Q. Lin).

https://doi.org/10.1016/j.cclet.2023.109281
1001-8417/

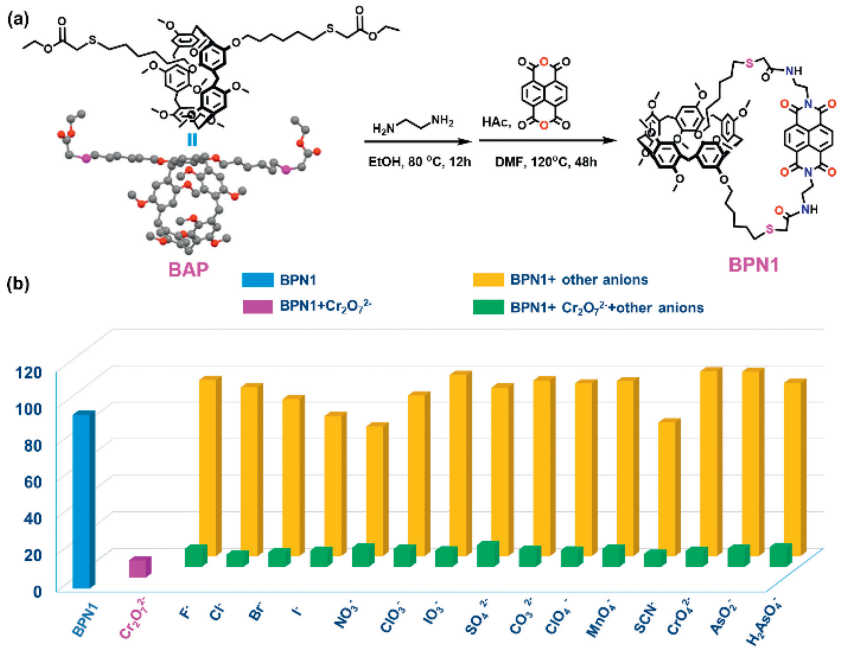

Fig. 1. (a) The single-crystal structure of **BAP** and synthesis of the fused bi-macrocyclic **BPN1**. (b) Fluorescence intensity ($\lambda_{ex} = 360$ nm, $\lambda_{em} = 425$ nm) of **BPN1** (1×10^{-4} mol/L) in the presence of various anions (50 equiv.) in DMSO/H_2O (9: 1, v/v).

In light of the above, herein, a novel fused bi-macrocyclic chemosensor molecule **BPN1** (Fig. 1a) has been rationally designed and synthesized. In **BPN1**, the electron-rich cavity of the pillar[5]arene was expected to bind the accompanying cation of the dichromate anions, meanwhile, the methoxy groups on the pillar[5]arene could supply multiple hydrogen bond interactions for $Cr_2O_7^{2-}$. In addition, the naphthalene-diimide (**NDI**) group and *N*-(2-amino-ethyl)-2-hexyl-thioethyl-amide moieties were employed to form a macrocycle with one phenyl group of pillar[5]arene. The obtained macrocycle possesses abundant supramolecular interaction sites, which also could bind other $Cr_2O_7^{2-}$ anions. Therefore, one fused bi-macrocyclic host molecule **BPN1** could bind several $Cr_2O_7^{2-}$ anions. This is an enrichment effect and could improve the sensitivity of $Cr_2O_7^{2-}$. As we expected, based on the enrichment effect, the fused bi-macrocyclic host molecule **BPN1** could detect $Cr_2O_7^{2-}$ with high selectivity and high sensitivity.

First, the pillar[5]arene-based fused bi-macrocyclic chemosensor **BPN1** was synthesized by the cyclization of **BAP** with **NDI** (Fig. 1a) and the obtained **BPN1** has been fully characterized (Figs. S10-S14 in Supporting information). Fortunately, a single crystal of ethyl mercapto-acetate functionalized pillar[5]arene (**BPA**) was obtained (Figs. S3-S5 in Supporting information). In the single crystal, the flexible chain of the **BPA** is on the outside of pillar[5]arene, which provides strong support for the flexible chain and **NDI** to form a ring on the outside of the pillar[5]arene. Furthermore, the size of the cavity of the pillar[5]arene is 5 Å [40], and the size of **NDI** is 6.62 Å [41]. Therefore, the obtained new ring is located on the outside of the pillar[5]arene cavity.

In order to test the enrichment effect of the **BPN1**, host-guest interactions were investigated by adding 50 equiv. of various anions (F^-, Cl^-, Br^-, I^-, NO_3^-, ClO_3^-, IO_3^-, SO_4^{2-}, CO_3^{2-}, ClO_4^-, MnO_4^{2-}, SCN^-, CrO_4^{2-}, $Cr_2O_7^{2-}$, AsO_2^-, $H_2AsO_4^-$, 0.1 mol/L, water solution) into the solution (DMSO/H_2O, 9:1, v/v) of **BPN1** (1×10^{-4} mol/L), respectively. As shown in Fig. 1b and Fig. S15 (Supporting information), only $Cr_2O_7^{2-}$ could induce the fluorescence decrease of the **BPN1** solution, while other anions could not induce a similar response. These results indicated that **BPN1** possesses selective recognition properties for $Cr_2O_7^{2-}$. In addition, in the presence of other anions (F^-, Cl^-, Br^-, I^-, NO_3^-, ClO_3^-, IO_3^-, SO_4^{2-}, CO_3^{2-}, ClO_4^-, MnO_4^-, SCN^-, AsO_2^-, and $H_2AsO_4^-$ (50 equiv.)), $Cr_2O_7^{2-}$ (50 equiv.) was added to **BPN1** (1×10^{-4} mol/L) and fluorescence experiments were carried out (Fig. S16 in Supporting information) [42]. The results show that the existence of the other anions does not interfere with **BPN1** recognition of $Cr_2O_7^{2-}$. According to competing experiments (Fig. 1b) and coexisting anions experiments, coexisting anions could not influence the $Cr_2O_7^{2-}$ recognizing process, which demonstrated the good anti-interference ability of **BPN1** on selective sensing $Cr_2O_7^{2-}$. Furthermore, according to the fluorescent titration experiments (Fig. S17 in Supporting information), with the gradual fluorescence intensity of the **BPN1** solution at 425 nm decreased by degrees. In addition, based on the fluorescence titration spectra and calculation *via* the $3\sigma/m$ method (Figs. S18-S20 in Supporting information) [43], the lowest limit of detection (LOD) of the **BPN1** to $Cr_2O_7^{2-}$ is 1.27×10^{-7} mol/L, which indicated that the **BPN1** has a high sensitivity for detection of $Cr_2O_7^{2-}$. Meanwhile, as shown in Table 1 [44–52], compared with reported $Cr_2O_7^{2-}$ sensing materials, the **BPN1** possesses considerably higher sensitivity.

To deeply understand the $Cr_2O_7^{2-}$ recognition mechanism of the fused bi-macrocyclic compound **BPN1**, a series of researches including HR-MS, ^1H NMR titration, FT-IR, SEM, as well as density functional theory (DFT) had been carried out. In the beginning, the HR-MS had been employed to evaluate the stoichiometry of the host-guest complexes, in the HR-MS (Fig. S22 in Supporting information), the negative ion pattern shows the peak at $m/z = 840.1957$, which agree with the [**BPN1**+ $K_2Cr_2O_7$ -H]$^{2-}$ and could be attributed to the **BPN1** forming an ions pair complex with $K_2Cr_2O_7$ (**BPN1**:$K_2Cr_2O_7$ = 1:1). Meanwhile, the peak at $m/z = 472.5684$ agree with the [**BPN1**+ $2Cr_2O_7$]$^{4-}$, which could be attributed to the formation of **BPN1**+ $2Cr_2O_7^{2-}$ complex (**BPN1**:$Cr_2O_7^{2-}$ = 1:2). Simultaneously, the peak at $m/z = 339.0240$ agree with the [**BPN1**+ $3Cr_2O_7$]$^{6-}$, which could be attributed to the formation of **BPN1**+ $3Cr_2O_7^{2-}$ complex (**BPN1**:$Cr_2O_7^{2-}$ = 1:3). These results show that the fused bi-macrocyclic compound **BPN1** can bind to multiple $Cr_2O_7^{2-}$ and have certain enrichment effect.

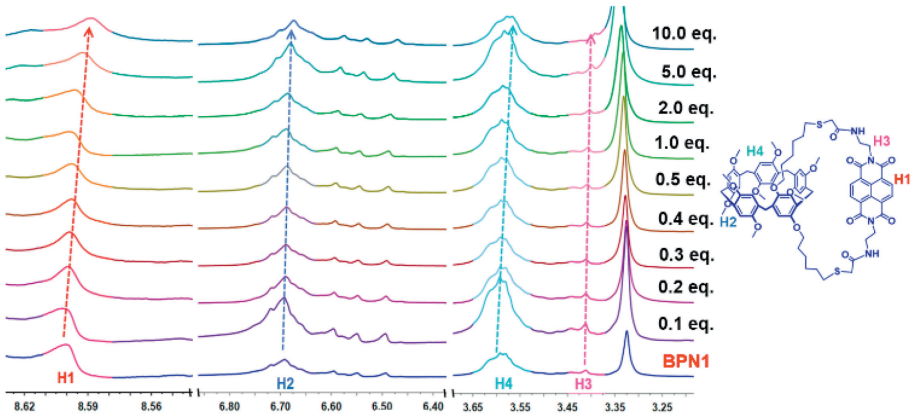

Fig. 2. ^{1}H NMR titration spectra (400 MHz, DMSO–d_6, 298 K) of **BPN1** and **BPN1** + $Cr_2O_7^{2-}$.

Table 1
Comparison of LOD with some reported of materials for $Cr_2O_7^{2-}$.

Materials	LOD (μmol/L)	Ref.
A multi-dye containing MOF	30	44
A bi-functional 3D Pb^{II}–organic framework	10.3	45
An unusual (3,4,5)-connected 3D cadmium metal–organic framework	2.16	46
A fluorescent metal-organic framework (MOF)	2.04	47
Chalcopyrite-type $CuFeSe_2$ nanocrystals	1.9	48
Zr(IV)-based metal-organic framework with t–shaped ligand	1.5	49
Based on lanthanide complex functionalized poly(ionic liquid)	0.68	50
Dual-functionalized fluorescent cationic organic network	0.65	51
Metal-organic frameworks hybrids with carbon dots	0.21	52
Chemosensor **BPN1**	0.12	This Work

In the ^{1}H NMR titration experiments (Fig. 2), after the gradual addition of 10 equiv. of $Cr_2O_7^{2-}$ into the **BPN1** solution, the proton signal of H_1 on the outer ring showed upfield shift, which is due to the anion-π interaction between the **NDI** group and $Cr_2O_7^{2-}$. In addition, the proton H_1 signal on the outer ring is also shifted upfield, indicating that there may be hydrogen bonds between the alkyl chain on the outer ring and $Cr_2O_7^{2-}$. Both H_2 and H_4 on the pillar[5]arene cavity are shifted to high fields, indicating that there may also be hydrogen bonds and anion-π interactions between the pillar[5]arene cavity and $Cr_2O_7^{2-}$. Moreover, in the corresponding FT-IR spectra, upon the addition of $Cr_2O_7^{2-}$ into the **BPN1**, the -NH signal shifted from 3398 cm^{-1} to 3427 cm^{-1}, while the C=O signal shifted from 1705 cm^{-1} to 1690 cm^{-1}. These shifts could be attributed to $Cr_2O_7^{2-}$ binding with -NH to form -N-H $Cr_2O_7^{2-}$ hydrogen bonds (Fig. S23 in Supporting information).

In order to deeply understand and visualization the binding mechanism of fused bi-macrocyclic compounds **BPN1** and $Cr_2O_7^{2-}$, the host-guest interaction was studied by density functional theory (DFT) [53]. First, a separate theoretical calculation of the host **BPN1** was performed, and isosurface maps of intramolecular interactions were obtained at ωB97XD/6–311+*G*(d, p) level [54,55]. All DFT calculations uses 6–311*G*(d, p) for **BPN1** and 6–311+*G*(d, p) for $Cr_2O_7^{2-}$ with implicit solvation model. The **BNPI** optimized structure is shown in Fig. 3a, and the **NDI** part of the side ring is parallel to the methoxybenzene part of the pillar[5]arene cavity. Using Multiwfn to visualize the weak intramolecular interaction of **BPN1** [56–58], it can be seen that this is due to the strong van der Waals force (π-π interaction) between the **NDI** on the side ring and the methoxybenzene part of the pillar[5]arene, the distance between the two paralleled groups is 3.4 Å (Fig. 3a). As shown in Fig. 3b, ESP (the electrostatic potential maps) of **BPN1** also shows that the methoxy group in the pillar[5]arene cavity and the alkyl chain on the side ring have a strong positive charge and are easy to combine with electron-rich groups such as anions. Meanwhile, the π plane and a large number of heteroatoms of the **NDI** ring on the side ring can provide abundant supramolecular interaction sites, forming anion-π interactions and multiple H-bond interactions.

Next, to deeply study the specific binding mode between the **BNP1** and the $Cr_2O_7^{2-}$, the DFT study was carried out based on the ^{1}H NMR titration and FT-IR spectra under different binding ratio of host and guest. As shown in Fig. 3, according to the DFT results, the relative positions of the host-guest binding were determined. It can be seen from Fig. 3a that the host-guest complex with a binding ratio of 1:2 has the least configuration change compared with the host **BPN1** alone. To understand the complexation mode of fused bi-macrocyclic host **BNP1** with the $Cr_2O_7^{2-}$ guest, a knowledge of the charge distribution and reactive sites is crucial and can be gauged through the ESP. Among the three different complexes formed by weak interactions, the electron density inside the cavity of the pillar[5]arenes was significantly decreased, thus allowing for the formation of new host- guest complexes with anionic guests *via* anion-π interactions (Fig. 3b). Besides, the frontier molecular orbitals (highest occupied molecular orbital and lowest unoccupied molecular orbital, HOMO, and LUMO) of the complexes with different host-guest binding ratios by DFT is obtained. In Fig. S24 (Supporting information), the HOMO orbital of **BPN1** is mainly distributed on the pillar[5]arene cavity. In [**BPN1** + $K_2Cr_2O_7$], the HOMO orbitals are mainly distributed in the pillar[5]arene cavity near the side ring, in addition, they are also distributed on the **NDI**. These changes are caused by the redistribution of electrons. The HOMO-LUMO gap of [**BPN1** + $K_2Cr_2O_7$] is 5.64 eV which is greater than **BPN1** (5.10 eV). In [**BPN1**+ $2Cr_2O_7^{2-}$], the LUMO orbital was transferred from the **NDI** portion of **BPN1** to the side ring, most likely because of the host-guest interaction between $Cr_2O_7^{2-}$ and the side ring. The frontier molecular orbitals also of [**BPN1**+ $3Cr_2O_7^{2-}$] are mainly distributed in pillar[5]arenes cavity and the HOMO-LUMO gap is 5.15 eV. On observing the values of the [**BPN1**+ $2Cr_2O_7^{2-}$] and [**BPN1**+ $3Cr_2O_7^{2-}$] molecules, [**BPN1**+ $2Cr_2O_7^{2-}$] are smaller than [**BPN1**+ $3Cr_2O_7^{2-}$]. All these results suggest that the [**BPN1**+ $2Cr_2O_7^{2-}$] have a greater affinity and thus have stronger interactions. In addition, to clearly demonstrate the strength of the interaction between the host and

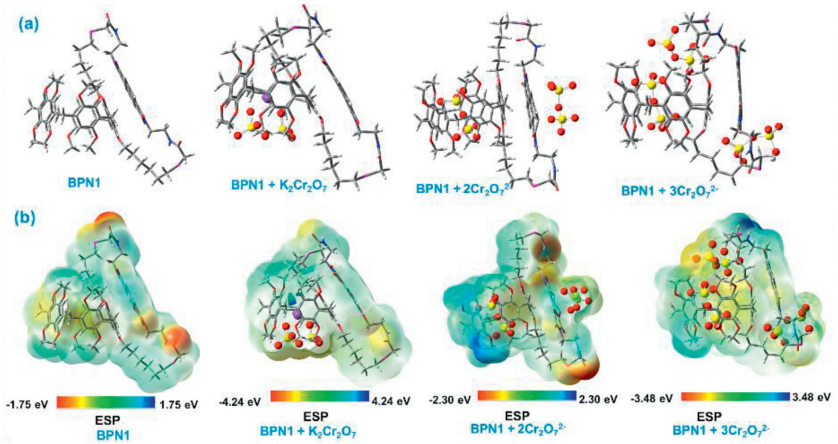

Fig. 3. (a) Side view the structure optimization. (b) The ESP (the electrostatic potential maps) of free **BPN1**, [**BPN1**+ $K_2Cr_2O_7$], [**BPN1**+ $2Cr_2O_7^{2-}$], [**BPN1**+ $3Cr_2O_7^{2-}$] at the ωB97XD/6–311+*G*(d, p) level.

Table 2
The total energy (*E*) of host (**BPN1**) and guest ($Cr_2O_7^{2-}$) and host-guest binding energies (*BE*).

BPN1:$Cr_2O_7^{2-}$	E_{host} (Hartree)	E_{gest} (Hartree)	$E_{Complex\ (H\text{-}G)}$ (Hartree)	Binding energies (kcal/mol)
1:1	-5204.806	-3815.538	-9020.485	-88.176
1:2	-5204.620	-5230.430	-10435.7763	-455.778
1:3	-5204.528	-7845.664	-13051.129	-588.031

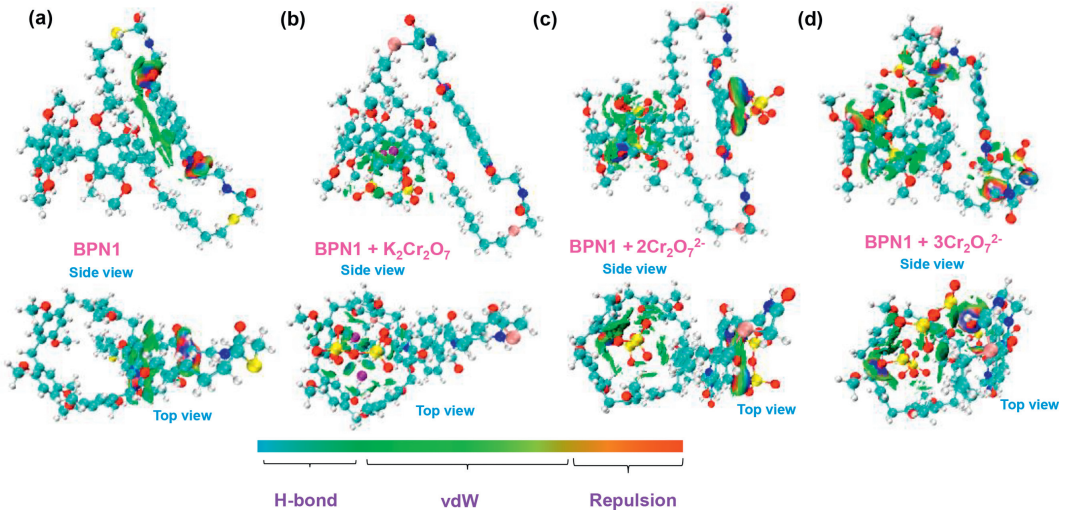

Fig. 4. IGMH analysis of (a) free **BPN1**, (b) [**BPN1**+ $K_2Cr_2O_7$], (c) [**BPN1**+$2Cr_2O_7^{2-}$], (d) [**BPN1**+$3Cr_2O_7^{2-}$] at the ωB97XD/6–311+*G*(d, p) level.

the guest, the binding free energy is also calculated. The binding free energies were obtained by subtracting the sum of individual host and guest self-consistent field energies from that of the complex [59]. As shown in Table 2, the binding free energies of **BPN1**+ $Cr_2O_7^{2-}$, **BPN1**+ $2Cr_2O_7^{2-}$, **BPN1**+ $3Cr_2O_7^{2-}$ are −88.76, −455.778, −588.031 kcal/mol, respectively. The results indicated that the binding free energies of **BPN1** and $Cr_2O_7^{2-}$ enhanced with increasing the binding ratio of **BPNI** and $Cr_2O_7^{2-}$. This result indicated that the binding of host and guest is more stable in a higher binding ratio, which agrees with the "enrichment effect".

For visually showing the multiple supramolecular interactions, the noncovalent interaction picture was got by the IGMH approach [60,61]. IGMH analysis has been performed by considering both guest molecules as the fragment and the host molecule as another one, and the obtained δg^{inter} green isosurface highlights the interaction region between the corresponding fragments (Fig. 4). The noncovalent interaction analysis can provide details to distinguish different weak noncovalent interactions, such as van der Waals, hydrogen bonds, and steric repulsion, and describe their intensity quantitatively. The color-coding scheme is as follows: red regions mean strong repulsive, strong attractive interactions are shown in blue while green regions represent electrostatic interactions. 3D isosurfaces and scatter diagrams for complexes are illustrated (Fig. S27 in Supporting information). These green patches are syllabified visualizing the interactions between **BPN1** and $Cr_2O_7^{2-}$, like anion-π interactions and multiple hydrogen bonds. The above results support our proposal of an "enrichment effect" in chemosensor design to enhance host-guest interaction.

Moreover, by SEM experiments with different ratios of host and guest, as shown in Fig. 5, **BPN1** exists in a regular spherical structure, while when 1 equiv. $Cr_2O_7^{2-}$ is added, **BPN1**+ $Cr_2O_7^{2-}$ shows agglomerated nanosphere structure; when 2 equiv. $Cr_2O_7^{2-}$ is added, **BPN1**+ $2Cr_2O_7^{2-}$ shows aggregated a three-

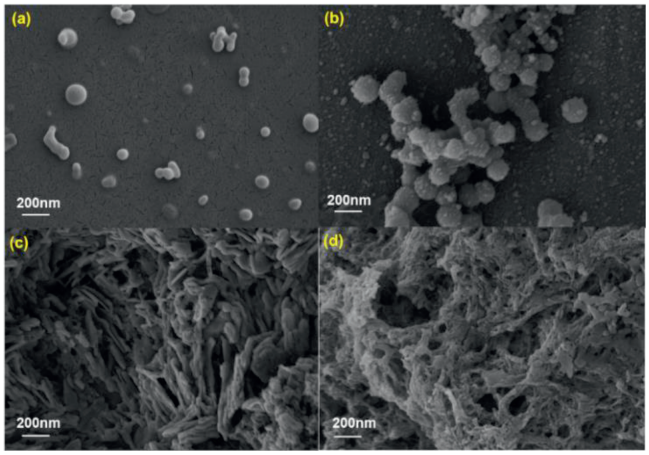

Fig. 5. SEM images showing the morphology of (a) **BPN1;** (b) **BPN1**+ $Cr_2O_7^{2-}$; (c) **BPN1**+ $2Cr_2O_7^{2-}$; (d) **BPN1**+ $3Cr_2O_7^{2-}$.

dimensional rod-like structure; while adding 3 equiv. $Cr_2O_7^{2-}$, **BPN1**+ $3Cr_2O_7^{2-}$ showed a three-dimensional sponge-like structure. With the increase of $Cr_2O_7^{2-}$, the host and guest are gradually crosslinked, and then the morphology changes from nanospheres to three-dimensional sponge network structure. These results clearly show that the bi-macrocyclic host **BPN1** and $Cr_2O_7^{2-}$ can bind by three different ratios, and the electron microscope morphology of the three binding modes can predict that different ratios of host-guest complexes have different modes of action. The above results were consistent with DFT calculations, and indicated that the "enrichment effect" in chemosensor design really enhanced the host-guest interactions.

In conclusion, a novel bi-macrocyclic chemosensor **BPN1** was synthesized and developed. The **BPN1** could highly sensitively and selectively recognize $Cr_2O_7^{2-}$ by the fluorometric response. The host and guest are gradually crosslinked, and then the morphology changes from nanospheres to three-dimensional sponge network recognition mechanism of **BPN1** toward $Cr_2O_7^{2-}$ was deeply studied by experiments and DFT. As a result, the sensitive and selective sensing mechanism of **BPN1** for $Cr_2O_7^{2-}$ was based on the enrichment effect which was supplied by the bi-macrocycle of the chemosensor **BPN1** through multiple intermolecular hydrogen bonding and electrostatic attractions. This work provided an easy way to improving the sensitivity and selectivity of chemosensor by inducing enrichment effect.

Declaration of competing interest

The authors declare that they have no known competing financial interests or personal relationships that could have appeared to influence the work reported in this paper.

Acknowledgments

This work was supported by the National Natural Science Foundation of China (NSFC, Nos. 22065031, 22061039, 22001214, 22165027), the top-notch talent project in Gansu province, the Key R & D Program of Gansu Province (No. 21YF5GA066), Gansu Province College Industry Support Plan Project (No. 2022CYZC-18), Natural Science Foundation of Gansu Province (Nos. 2020–0405-JCC-630, 20JR10RA088), The star of innovation (No. 2023CXZX-244).

Supplementary materials

Supplementary material associated with this article can be found, in the online version, at doi:10.1016/j.cclet.2023.109281.

References

[1] J. Tian, X. Hu, Z. Hu, Nat. Commun. 13 (2022) 4293-4205.
[2] R. Cen, M. Liu, J. He, et al., Chin. Chem. Lett. 34 (2023) 108195–108200.
[3] S. Sevim, A. Sorrenti, C. Franco, et al., Chem. Soc. Rev. 47 (2018) 3788–3803.
[4] Y. Meng, Y. Liu, Z. Wan, et al., Chem. Eng. J. 453 (2023) 139967–139975.
[5] Q. Liang, B. Shao, S. Tong, et al., Chem. Eng. J. 405 (2021) 126951–126976.
[6] Y. Jia, J. Li, Acc. Chem. Res. 52 (2019) 1623–1631.
[7] C. Tu, W. Wu, W. Liang, et al., Angew. Chem. Int. Ed. 61 (2022) e202203541.
[8] B. Li, Q. Xu, X. Shen, et al., Chin. Chem. Lett. 34 (2023) 108015.
[9] R. Kumar, A. Sharma, H. Singh, et al., Chem. Rev. 119 (2019) 9657–9721.
[10] X. Zhang, S. Tong, J. Zhu, et al., Chem. Sci. 14 (2023) 827–832.
[11] P. Li, Y. Chen, Y. Liu, Chin. Chem. Lett. 30 (2019) 1190–1197.
[12] H. Nie, Z. Wei, X.L. Ni, et al., Chem. Rev. 122 (2022) 9032–9077.
[13] H. Liang, Y. Yang, L. Shao, et al., J. Am. Chem. Soc. 145 (2023) 2870–2876.
[14] H. Liang, B. Hua, F. Xu, et al., J. Am. Chem. Soc. 142 (2020) 19772–19778.
[15] Y. Li, X. Lou, C. Wang, et al., Chin. Chem. Lett. 34 (2023) 107877.
[16] Y.J. Li, T.T. Huang, J. Liu, et al., ACS Sustainable Chem. Eng. 10 (2022) 7907–7915.
[17] M. Li, Y. Liu, L. Shao, et al., J. Am. Chem. Soc. 145 (2023) 667–675.
[18] K. Wang, M. Zuo, T. Zhang, et al., Chin. Chem. Lett. 34 (2023) 107848.
[19] B. Jiang, W. Wang, Y. Zhang, et al., Angew. Chem. Int. Ed. 56 (2017) 14438–14442.
[20] J.R. Wu, G. Wu, D. Li, et al., Angew. Chem. Int. Ed. 62 (2023) e202218142.
[21] L. Chen, Y. Wang, Y. Wan, et al., Chem. Eng. J. 387 (2020) 124087–124097.
[22] K. Kato, S. Fa, S. Ohtani, et al., Chem. Soc. Rev. 51 (2022) 3648–3687.
[23] J.R. Wu, G. Wu, Y.W. Yang, et al., Acc. Chem. Res. 55 (2022) 3191–3204.
[24] C. Xiao, W. Wu, W. Liang, et al., Angew. Chem. Int. Ed. 59 (2020) 8094–8098.
[25] J. Yao, W. Wu, C. Yang, et al., Nat. Commun. 12 (2021) 2600–2609.
[26] E. Lee, H. Ju, S.S. Lee, et al., J. Am. Chem. Soc. 140 (2018) 9669–9677.
[27] W.B. Hu, H.M. Yang, W.J. Hu, et al., Chem. Commun. 50 (2014) 10460–10463.
[28] Y. Lv, C. Xiao, J. Ma, et al., Chin. Chem. Lett. 35 (2024) 108757.
[29] W.B. Hu, W.J. Hu, X.L. Zhao, et al., Chem. Commun. 51 (2015) 13882–13885.
[30] V. Singh, N. Singh, S.N. Rai, et al., Toxics 11 (2023) 147.
[31] C. Ding, Y. Deng, A. Merchant, et al., Sep. Purif. Rev. 52 (2023) 123–134.
[32] Q. Huang, Y. Zhang, W. Zhou, et al., Chin. Chem. Lett. 32 (2021) 2797–2802.
[33] C. Bai, J. Zhang, Y. Qin, et al., Anal. Chem. 94 (2022) 11298–11306.
[34] W. Wu, N.J. Planavsky, Chem. Geol. 456 (2017) 98–111.
[35] M. Costa, C.B. Klein, Crit. Rev. Toxicol. 36 (2006) 155–163.
[36] J. Sun, P. Guo, M. Liu, et al., J. Mater. Chem. C 7 (2019) 8992–8999.
[37] X. Li, L. Jin, L. Huang, et al., J Environ. Chem. Eng. 9 (2021) 106357–106366.
[38] R.J. Satya, C. Joyanta, J. Haz. Mat. 405 (2021) 124242–124251.
[39] X. Zhang, X. Wang, W. Fan, et al., Mater. Chem. Front. 4 (2020) 1150–1157.
[40] T. Ogoshi, S. Kanai, S. Fujinami, et al., J. Am. Chem. Soc. (13) (2008) 5022–5023.
[41] D.E. Zacharias, Acta Cryst. C 49 (1993) 1082–1087.
[42] M.M. Xu, X.J. Kong, T. He, et al., Inorg. Chem. 57 (2018) 14260–14268.
[43] A.M. Committee, Analyst 112 (1987) 199–204.
[44] J. Yoo, U. Ryu, K.M. Choi, Sensor Actuat B: Chem 283 (2019) 426–433.
[45] M.C. Lin, Inorg. Chem. Commun. 105 (2019) 86–92.
[46] J.X. Li, D. Liu, Z.C. Hao, et al., Inorg. Chem. Commun. 97 (2018) 79–82.
[47] H.N. Chang, L.W. Liu, Z.C. Hao, et al., J. Mol. Struct. 1155 (2018) 496–502.
[48] N. Wu, Y. Li, M. Zeng, et al., Solid State Chem. 271 (2019) 292–297.
[49] T. He, Y.Z. Zhang, X.J. Kong, et al., ACS Appl. Mater. Interfaces 10 (2018) 16650–16659.
[50] H. Dang, H. Zou, S. Liu, et al., Dyes Pigments 172 (2020) 107804–107812.
[51] Z.J. Li, Y.X. Ma, Q. Zhang, ACS Appl. Mater. Interfaces 11 (2019) 46197–46204.
[52] Y. Wang, J. He, W. Wei, Talanta 191 (2019) 519–525.
[53] M.J. Frisch, G.W. Trucks, H.B. Schlegel, et al., J. GAUSSIAN 09, Revision D.01, (Gaussian Inc.: Wallingford CT, 2013).
[54] W. Humphrey, A. Dalke, K. Schulten, J. Molec. Graphics 14 (1996) 33–38.
[55] M.J. Frisch, J.A. Pople, J.S. Binkley, J. Chem. Phys. 80 (1984) 3265–3273.
[56] T. Lu, F.W. Chen, J. Comput. Chem. 33 (2012) 580–592.
[57] J. Rak, P. Skurski, J. Simons, et al., J. Am. Chem. Soc. 123 (2001) 11695–11707.
[58] D.P. Malenov, S.D. Zarić, Chem. Eur. J. 27 (2021) 17862–17872.
[59] W. Charles Jr., Bauschlicher, Chem. Phys. Lett. 694 (2018) 86–92.
[60] C. Lefebvre, G. Rubez, H. Khartabil, et al., Chem. Chem. Phys. 19 (2017) 17928–17936.
[61] T. Lu, Q. Chen, J. Comput. Chem. 43 (2022) 539–555.